Control of Protein Activity and Cell Fate Specification via Light-Mediated Nuclear Translocation

Hayretin Yumerefendi , Daniel J. Dickinson , Hui Wang , Seth P. Zimmerman, James E. Bear, Bob Goldstein, Klaus Hahn , Brian Kuhlman

Published: June 17, 2015 • http://dx.doi.org/10.1371/journal.pone.0128443

Abstract

Light-activatable proteins allow precise spatial and temporal control of biological processes in living cells a approaches have been developed for controlling protein localization with light, including the conditional inh localization signal (NLS) with the Light Oxygen Voltage (AsLOV2) domain of phototropin 1 from *Avena sat* switch adopts a closed conformation that sterically blocks the NLS motif. Upon activation with blue light th protein unfolds, freeing the NLS to direct the protein to the nucleus. A previous study showed that this app control the localization and activity of proteins in mammalian tissue culture cells. Here, we extend this resu binding properties of a LOV/NLS switch and demonstrating that it can be used to control gene transcriptio we show that the switch, referred to as LANS (light-activated nuclear shuttle), functions in the *C. elegans* e control of nuclear localization in individual cells. By inserting LANS into the *C. elegans lin-1* locus using Ca recombination, we demonstrated control of cell fate via light-dependent manipulation of a native transcripti that LANS can be a valuable experimental method for spatial and temporal control of nuclear localization *i*

Citation: Yumerefendi H, Dickinson DJ, Wang H, Zimmerman SP, Bear JE, Goldstein B, et al. (2015) C Activity and Cell Fate Specification via Light-Mediated Nuclear Translocation. PLoS ONE 10(6): e0128 doi:10.1371/journal.pone.0128443

Academic Editor: Alexander F. Palazzo, University of Toronto, CANADA

Received: February 27, 2015; **Accepted:** April 27, 2015; **Published:** June 17, 2015

Data Availability: All relevant data are within the paper and its Supporting Information files.

Funding: This work was supported by NIH grants R01 GM093208 (B.K.), R01 DA036877 (B.K, K.H), R R01 GM102924 (K.H.), and T32 CA009156 (D.J.D.); and by Howard Hughes postdoctoral fellowship fr Whitney Foundation (D.J.D.); H.W. is a recipient of an Arthritis Foundation Postdoctoral Fellowship. Th in study design, data collection and analysis, decision to publish, or preparation of the manuscript.

Competing interests: The authors have declared that no competing interests exist.

Introduction

Many biological processes rely on the precise spatial segregation of macromolecules within a living cell. R partitioning is a common mechanism for controlling gene expression through sequestering transcription fa Analogously, inducible nucleocytoplasmic translocation represents a powerful approach to control cell beh removing a protein of interest from the cellular compartment where it is active. We sought to generate a si genetically encoded and reversible light-driven nuclear import switch. We hypothesized that it would allow genes of interest in a variety of experimental systems, including multicellular organisms.

Protein engineering in combination with small molecules has previously been used to control nucleocytopl examples of experimental tools for conditional nuclear import have used the nuclear hormone receptor Es which is cytoplasmic until bound to its ligand. This approach was first applied to control the Myc transcripti improved version that makes use of the estrogen receptor antagonist tamoxifen has been widely used for recombination with the Cre recombinase (Cre-ER^T) [3, 4]. Anchor-Away is a two-component system that v protein of interest in the cytosol via rapamycin-dependent heterodimerization between FKBP12 and the FF mTOR kinase. One is fused to a ribosomal protein and the other to the protein of interest [5]. These appro chemical molecules tamoxifen and rapamycin for induction. Chemical induction requires that small molecu biological tissue, has limited reversibility and lacks fine spatial control in an organism.

Optogenetic tools are minimally invasive, allow for subcellular spatial control, and have reversible, rapid a time scales from milliseconds to hours [6]. Transparent model organisms such as the nematode *C*. *elegan* and the zebrafish *D*. *rerio* are especially well suited for optogenetics, and photoactivatable proteins have e these systems unattainable with conventional techniques [7–9]. Light-activated control of nuclear import re potentially general way of controlling multiple cellular functions.

Deiters and co-workers controlled protein localization by incorporating a photoactive amino acid in a nucle that it could only interact with the nuclear import machinery when the chemical moiety was removed via irr 11]. This approach is not reversible and requires the bioavailability of a non-natural amino acid. Equivalent technique is a recently developed organelle targeting system that uses the red light mediated interaction b (PhyB) and phytochrome-interacting factor 6 (PIF6) [12]. The association and dissociation kinetics of this s has been used to study the effects of the mitotic cyclin Clb2 in nuclear fission and spindle stabilization in y requirement for a non-natural cofactor (PCB) presents an obstacle to the use of this system in living anima

Very recently the first fully optogenetic tool for the control of nuclear import was reported by Niopek and co engineered switch makes use of the LOV2 domain from *Avena Sativa* (AsLOV2). When activated with blu domain undergoes a conformational change and the C-terminal Jα helix unfolds. To control nuclear localiz embedded at the end of the Jα helix so that it is sterically hindered from binding the nuclear import machir in its closed, dark-state conformation. Upon activation with light, the NLS becomes accessible and the pro nucleus. To make the switch reversible, a constitutive NES was added to direct the protein to the cytoplasi hidden in the dark state. It was shown that it was important to tune the relative strengths of the NLS and N the dynamic range of the switch. To demonstrate functional activity, the switch was used to control transcri in mammalian cells.

Here, we confirm and extend the findings of Niopek et al. [13] and present the design, engineering and ap Activated Nuclear Shuttle (LANS) that also makes use of the AsLOV2 domain to cage a NLS motif. We dir functions by regulating its binding affinity to variants of importin α. LANS allows for robust control of transc exhibits fast blue light-induced nuclear import as well as dark cytoplasmic reversion in a variety of mamma CRISPR/Cas9-mediated insertion of LANS into the *lin-1* gene of *C*. *elegans* conferred light dependence o transcription factor, allowing optogenetic control of vulval cell fate specification in living animals.

Results

Design of a light-conditioned nuclear localization signal

To control nuclear import with light we engineered a conditional Nuclear Localization Signal (cNLS) that w blocked in the dark but available for binding to importin in the light (Fig 1A). Previously, the AsLOV2 doma

been successfully used to control the binding of short, linear sequence epitopes [14–16] and does not con
nuclear localization signal. Therefore, to generate an allosterically caged NLS, we first attached the humai
the AsLOV2 domain after residue 546, aligning the proline residue from the NLS sequence to the proline r
fusion protein (AsLOV2cMyc) bound importin α5 with low nanomolar affinity and showed no light-depende
we decided to embed the Myc NLS further into the Jα helix, aligning the alanine residues present in both s
eliminate the conserved proline residue at the beginning of the NLS, which could disrupt the helicity of the
simulations with the modeling program Rosetta using the karyopherin-Myc NLS complex structure (PDB: 1
the proline residue of the Myc NLS to vary and identified a favorable methionine substitution (Fig 1B and S
used to build a model of the designed NLS sequence, grafted onto the AsLOV2 structure (PDB: 2v0u) cre
designed methionine pointed towards solvent, not clashing with any residues from the AsLOV2 domain, a
hydrophobic residues present in the NLS were well packed against the core PAS domain (S1 Fig).

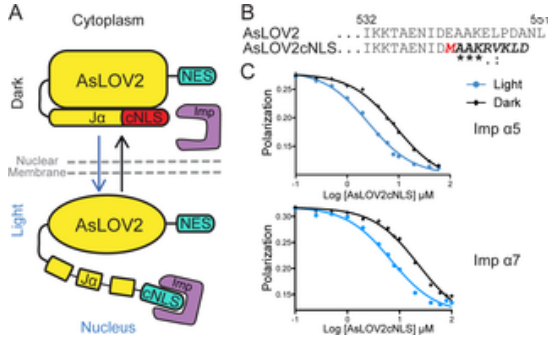

Fig 1. Design and biophysical characterization of light conditioned nuclear localization signal.
(A) Schematic of the Light Activated Nuclear Shuttle (LANS) design for light activated nuclear import (B
of the wild type AsLOV2 and the designed AsLOV2cNLS (sequence identity and homology is marked a
CLUSTALW scheme). (C) Fluorescence polarization competitive binding assay of AsLOV2cNLS agains
and importin α7.
http://dx.doi.org/10.1371/journal.pone.0128443.g001

The switch binds similarly to two distinct importins

Nuclear import efficiency is directly correlated to the binding affinity of a nuclear localization signal for impo
the binding affinities of the conditioned NLS for human importin α, we adopted a competition-based fluores
[14]. We expressed the AsLOV2cNLS construct and human importins in bacteria, purified them and meas
for both importins α5 and α7 under blue light irradiation (250 nM and 340 nM, respectively). Their affinities
decreased to 1.5 μM for importin α5, and 2 μM for importin α7, which represented a 6-fold change in light/
S2 Fig). Since efficient nuclear localization requires an importin binding affinity tighter than 1 μM [17], thes
predictive of efficient nuclear import upon light stimulus and reduced translocation in its absence. The simi
two distinct importin α proteins implies that the switch's nuclear translocation could be mediated by more t
Lastly, we tested whether the chimeric sequence affects the AsLOV2 photocycle. We observed that the da
AsLOV2cNLS does not deviate from that of wild type AsLOV2, with an activated state half-life of 29.5 sec

A Nuclear Export Signal is required for the reversible control of nuclear import

To determine whether the AsLOV2cNLS switch could control nuclear localization in live cells, we fused it t
protein and observed its sub-cellular distribution in HeLa cells (Fig 2A). In the dark the mCherry fluorescer
evenly distributed throughout the cells (Fig 2C top leftmost panel). Incorporating a well-studied AsLOV2 p
mimics its lit conformation [18] caused the mCherry signal intensity to concentrate in the nucleus, validatin
bottom leftmost panel). Since the nuclear pore complex allows passive diffusion of proteins with molecular
[19, 20], we hypothesized that the observed dark state distribution of the 45 kDa mCherry::AsLOV2cNLS p
passive diffusion throughout the cell, and that adding a nuclear export sequence (NES) could shift its distr
Hence, we needed to identify the appropriate balance between nuclear import and export signal strength,

NES would be sufficient to remove the switch from the nucleus in the dark but would be overpowered by tl conditional NLS in the light. We screened a panel of five NES sequences that vary in export strength and a nucleocytoplasmic shuttling proteins: PKI-α [21], p53 [22], Mdm2 [23], Smad4 [24] and p120ctn [25] (Fig 2 the NES sequences between mCherry and either the wild type or I539E switch variant. For each of the NE the nuclear/cytoplasmic distribution for either the wild type protein in the dark or the lit mimetic, which allov state distributions without concerns about the precise mode and timing of light stimulation. While the switc 2.64-fold increase in nuclear localization with the lit mimetic, some amount of protein was always present i = 1.35 ± 0.07 nuclear/cytoplasmic fluorescence, n = 10 and Lit mimetic = 3.57 ± 0.20 nuclear/cytoplasmic 2C and 2D). Three of the NES sequences provided lower nuclear fluorescence in the dark, p120ctn, PKI-α However, the NES motif from p120ctn was so strong that nuclear localization was not observed with the lit change in nuclear/cytoplasmic fluorescence (6.2 fold) was observed with the NES from Smad4 (Dark state nuclear/cytoplasmic fluorescence, n = 10 and Lit mimetic = 2.81 ± 0.19 nuclear/cytoplasmic fluorescence,

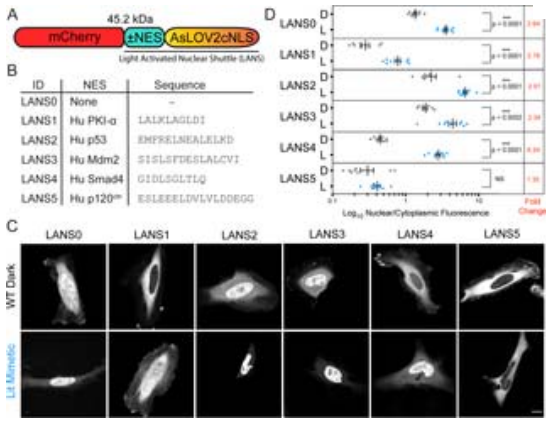

Fig 2. Confocal microscopy of LANS in HeLa cells.

(A) Schematic of the LANS constructs (B) List of the nuclear export signals tested. (C) Representative i cells used for the quantification of the nuclear/cytoplasmic distribution of the switch (scale bar = 15 μm) the effect of the nuclear export signal on the nuclear/cytoplasmic distribution of LANS (D—wild type cor dark, L—lit mimetic I539E). Mean is reported ±SEM and statistical significance calculated with unpairec test; NS—Not Significant.

http://dx.doi.org/10.1371/journal.pone.0128443.g002

To confirm that exclusion of the constructs from the nucleus required active nuclear export, we treated cell Leptomycin B [26]. Leptomycin B treatment led to loss of nuclear exclusion and restoration of the no-NES distribution for all but the p53 and Mdm2 NES (S3 Fig), indicating that the switch constitutively shuttles be the cytoplasm, and confirming that its nuclear export is mediated by Crm1. We therefore named the AsLO with an NES the Light Activatible Nuclear Shuttle (LANS). Here, we refer to different LANS constructs by a denotes the NES used: LANS0 carries no NES, while LANS1-5 use the nuclear export signals of PKI-α, p5 p120ctn, respectively (Fig 2B). LANS remains functional when short peptide or large globular proteins are (S3 Fig).

LANS is imported and exported within minutes in a variety of mammalian cell cultures

We next sought to characterize the kinetics of nuclear import and export in response to light stimulation. W stimulation and measured the rates of nuclear import and dark reversion for LANS4 in three types of mam cells—HeLa, Cos7 and HEK293 (Fig 3A, 3B and S1–S3 Movies). Nuclear fluorescence upon activation wa changes of nuclear accumulation were fit by single exponentials with $t_{1/2}$ = 3.3 ± 0.02 minutes for HeLa (n minutes for Cos7 (n = 3) and $t_{1/2}$ = 5.9 ± 0.01 minutes for HEK293 (n = 5) (Fig 3C). Upon stopping the blu nuclear export kinetics were similarly measured and fit, yielding $t_{1/2}$ = 2.5 ± 0.01 minutes for HeLa, $t_{1/2}$ = 2 Cos7 and $t_{1/2}$ = 3.2 ± 0.02 minutes for HEK293 (Fig 3C). The differences observed between the cell types differential expression of importins and exportins [27]. Nuclear localization appeared fully reversible, with r

activation level after multiple cycles of blue light activation and reversion over the course of a few hours (F

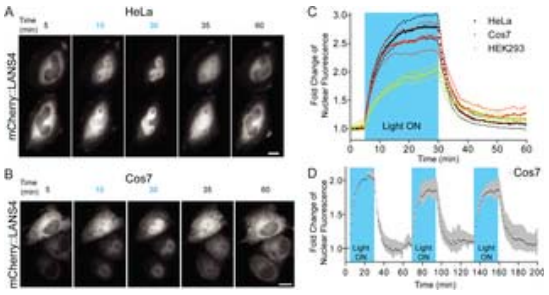

Fig 3. Real time light induced nuclear translocation of LANS4 in mammalian tissue culture cells.
(A) Representative images for light activation and reversion in HeLa cells and Cos7 (B) (scale bar = 25
fold change of nuclear accumulations in HeLa, Cos7 and HEK293 (n = 4 each, mean reported ± SEM w
also S1, S2 and S3 Movies. The blue shaded region indicates pulsed blue light activation (see Supplem
procedures). (C) Multple activation reversion cycles in Cos7 (n = 2, mean reported ± SEM with shaded
shaded regions indicate pulsed blue light activation.
http://dx.doi.org/10.1371/journal.pone.0128443.g003

LANS enables robust transcriptional control in yeast

To determine whether LANS could be used to control protein function in cells, we sought light-mediated cc
yeast. We used the NMY51 yeast strain (Fig 4A) and an NLS reported plasmid system [28] to which we fu
C-terminus (Fig 4B). Colony growth assays showed light-dependent survival when grown on media lacking
with no background detected for the vector (Fig 4C). Normal yeast growth was not affected by blue light (F
minus leucine). We then grew liquid cultures in light and dark and performed β-galactosidase assays to qu
transcriptional activation. A 21-fold change in signal was observed (8.8 ± 0.7 Miller Units (n = 3) in the dar
Units (n = 3) in the light). No detectable transcription was seen for a construct with a mutated conditional r
where all lysines and arginines were substituted with alanines (MAAAAVALD). These data demonstrate th
control the activity of a transcription factor by regulating its nuclear localization.

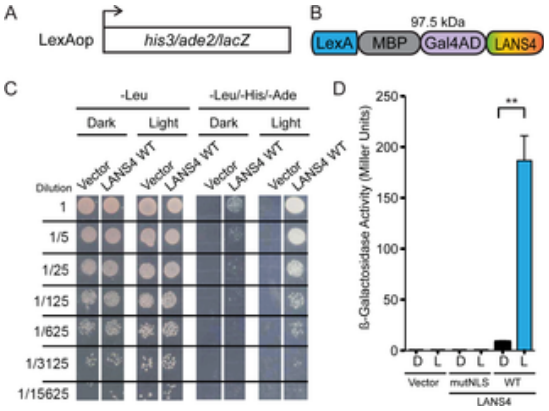

Fig 4. Light induced transcription via light mediated nuclear translocation in yeast.
(A) NMY51 contains *his3*, *ade2* and *lacZ* genomic reporter genes under the control of LexAop. (B) Sche
controlled artificial transcription factor in yeast (C) Growth assay of LANS controlled transcription factor
panel shows growth on media lacking leucine, which confers plasmid resistance and demonstrates that
not affect regular yeast growth. The right panel demonstrates light dependent growth on media lacking
adenine. (D) β-galactosidase activity measurements upon blue light induced transcription activation wit
mean reported ± SEM and statistical significance is calculated with unpaired two-tailed t-student's test (

http://dx.doi.org/10.1371/journal.pone.0128443.g004

LANS can be used to precisely control nuclear translocation in *C. elegans* embryos

To test whether LANS can be used to regulate protein nuclear localization *in vivo*, we took advantage of th of genetic manipulation of the *C. elegans* embryo. We fused LANS4 to the red fluorescent protein mKate2 in *C. elegans* embryos under the control of the *his-72* promoter and *tbb-2* 3'UTR. This promoter and 3'UTI expression throughout development, with the strongest expression in developing embryos ([29] and D.J.D observations). The fusion protein was cytosolic in embryos kept in the dark, but translocated rapidly (< 2 n upon blue light activation (Fig 5B and S4 Movie). It returned fast (< 3 minutes) to the cytosol after the illum Expression and photoactivation of LANS did not appear to cause toxicity, since the embryos continued de hatched into viable L1 larvae after the experiment (n = 8 embryos from 2 separate experiments). We next achieve precise spatial control of nuclear translocation by targeting photoactivation to a single cell. For the embryos expressing mKate2::LANS4 in mesodermal precursors of the MS cell lineage under the control o [30]. Illumination of a cell expressing mKate2::LANS4 resulted in rapid nuclear translocation, which was re illumination was stopped (Cell 1 in Fig 5C and 5D and S5 Movie). No change in mKate2::LANS4 localizati neighbouring cell that was not illuminated (Cell 2 in Fig 5C and 5D and S5 Movie). The activation and reco by single exponentials with $t_{1/2}$ = 49 ± 9 seconds for activation and $t_{1/2}$ = 67 ± 9 for recovery (n = 11 exper that LANS can be used to control nuclear localization with high temporal and spatial precision in a living *C*

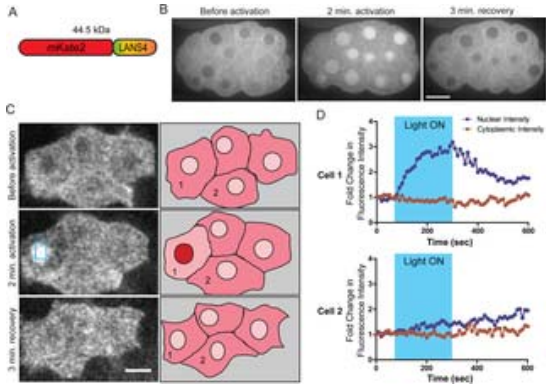

Fig 5. Light activated nuclear translocation in *C. elegans* embryo.
(A) Schematic of the mKate2::LANS construct that was expressed in *C. elegans* embryos (B) Confocal expressing mKate2::LANS ubiquitously and subjected to photoactivation with blue light. Scale bars repr S4 Movie. (C) Left: Confocal images of four mKate2::LANS expressing MS lineage cells on the ventral gastrulation-stage embryo. The blue box in the center image indicates the region that was photoactivat Brightness and contrast were adjusted to compensate for photobleaching. Scale bar represents 5 μm. I summarizing the observed localization. Numbers correspond to the cell numbers in (D). See also S5 M of nuclear and cytoplasmic fluorescence intensities as a function of time for the two cells labelled in (C) with blue light, and Cell 2 is a neighboring cell. These measurements were corrected for photobleachin methods).
http://dx.doi.org/10.1371/journal.pone.0128443.g005

LANS can be used to manipulate cell fate *in vivo*

To test whether LANS could be used to control the activity of a protein *in vivo*, we sought to manipulate the *elegans* vulva, a classical model system for studying cell fate specification [31]. During the third larval stag cells with equivalent developmental potential can be induced to adopt either primary or secondary vulval fa EGF signal from the nearby anchor cell. In wild type animals, a single cell called P6.p receives the stronge the primary vulval fate. Its neighbors, P5.p and P7.p, adopt the secondary vulval fate in response to a wea anchor cell together with a Notch signal from P6.p [31]. The remaining 3 precursor cells normally adopt nc

mutations in the EGF/Ras/Raf/MAPK signalling pathway cause ectopic induction of the primary vulval fate (Muv) phenotype. Loss-of-function mutations in this pathway impair vulval induction and cause a Vulvales

The LIN-1/ETS transcription factor is a downstream target of the MAPK pathway and is thought to functior primary vulval fate (Fig 6A). Strong *lin-1* loss of function mutations cause all six vulval cells to adopt prima fates, independent of the activity of the MAPK pathway, resulting in a strong Multivulval phenotype [32–34 function mutations in *lin-1* result in repression of the primary vulval fate [35]. MAPK phosphorylates LIN-1 C-terminal tail (Fig 6B), which inactivates LIN-1 and allows cells to adopt the primary vulval fate [35].

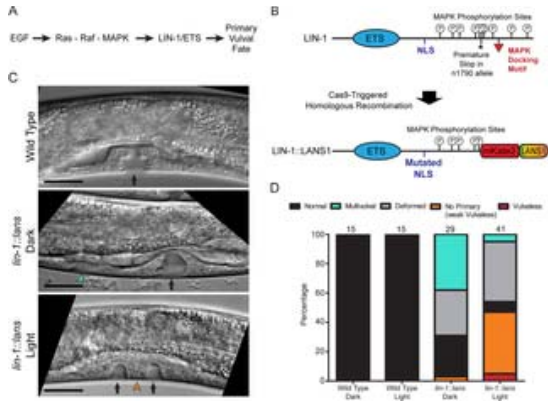

Fig 6. Control of vulval development via photoactivatable LIN-1.

(A) Simplified schematic of the role of LIN-1 in vulval fate specification. (B) Top: Schematic of the wild ty Bottom: Schematic of the LIN-1::LANS protein produced after modification of the native *lin-1* locus usin homologous recombination. See also S4 Fig. (C) DIC Images of the developing vulvae in mid-L4 larvae strains and conditions. Top panel: Black arrow indicates the normal, symmetric vulval invagination. Mid indicates the main vulval invagination, and green arrowhead indicates an extra vulval invagination. Bott arrowheads indicate small invaginations produced by the secondary vulval precursors, and black arrow tissue derived from the failed primary cell. Scale bars represent 20 μm. (D) Quantification of phenotype strains and conditions. See Methods for detailed definitions of each phenotype. Numbers at the top of e total number of animals scored in this experiment. These data are from a single experiment; the experi three times, using two independently isolated *lin-1*::*lans* alleles, with similar results.

http://dx.doi.org/10.1371/journal.pone.0128443.g006

To generate a light-inducible *lin-1* allele, we modified the endogenous *lin-1* gene using Cas9-triggered hon [36]. We introduced three molecular changes, with the goal of eliminating the normal regulation of LIN-1 b with optogenetic regulation (Fig 6B and S4 Fig). First, we truncated the C-terminus, mimicking the *n1790* g eliminates the MAPK docking site and most of the predicted phosphorylation sites [35]. Second, we mutat NLS. Third, we inserted sequence encoding mKate2::LANS1. We predicted that the resulting LIN-1::LANS sequestered in the cytosol and inactive in the dark, but would localize to the nucleus and be constitutively

We examined the phenotypes of *lin-1*::*lans1* animals raised in the dark or under blue light. Continuous illu no effect on the development of wild type animals (Fig 6C and 6D and DJD, unpublished observations), in levels used in this experiment were non-toxic. A substantial fraction (38%) of *lin-1*::*lans1* animals raised in Multivulval phenotype, consistent with our prediction that LIN-1::LANS1 should have reduced activity in th However, it is important to note that this phenotype is less severe and less penetrant than that of *lin-1* null suggesting that LIN-1::LANS1 retains some activity in the dark. This residual activity may be due to shuttli above), which results in the LIN-1::LANS1 transient nuclear localization even in the dark.

Illumination with blue light efficiently suppressed the Multivulval phenotype of *lin-1*::*lans1* animals (5% Mu exact test), indicating that LIN-1::LANS1 was activated by blue light. In addition, we observed animals that vulval invagination, a plug of tissue flanked by two smaller-than-normal invaginations (Fig 6C). We interpre Vulvaless phenotype, in which specification of the primary cell fails, but the secondary cells still invaginate

observed significantly more frequently in animals raised under blue light (Fig 6D; 42% vs. 3%; p = 0.0002, suggesting that light-activated LIN-1::LANS1 repressed the primary vulval fate, as predicted. Consistent w the weak Vulvaless phenotype, a small fraction (5%) of *lin-1*::*lans1* animals raised under blue light were co 6D). It is important to note that the *n1790* mutation, on which *lin-1*::*lans1* was modelled, produces a simila phenotype, with 54% of *n1790* animals showing vulval defects [35]. The penetrance of Vulvaless / weak V *lin-1*::*lans1* animals raised under blue light (54%) is similar to the penetrance of vulval defects in *n1790* an these data indicate that insertion of the LANS1 coding sequence into the *lin-1* gene allowed optogenetic c transcription factor and manipulation of cell fate decisions in a living animal.

Discussion

The LANS switch exhibits light dependent binding to both importin α 5 and importin α 7, indicating that mu can mediate its nuclear import. Although the switch accumulates in the nucleus upon light stimulation, in th passive diffusion through the nuclear pore complex results in even nuclear/cytoplasmic distribution in the d switch out of the nucleus in the dark, we coupled the switch with a constitutive nuclear export signal, which Crm1 for its function. Modulating the strength of the nuclear export signal permits tuning the nuclear/cytop protein of interest. The switch is further tunable using previously reported AsLOV2 dark state stabilizing m works in a range of mammalian tissue culture cells with similar kinetics, which lead to fast nuclear import a remains functional after hours of cycled activation and reversion, with the protein returning to initial nuclea stimulation is stopped.

In several ways our results provide independent confirmation of the findings of Niopek et al. [13] in their us to control nuclear import. Like us, they found it necessary to test different NES and NLS signals in order to range of their switch. Their best performing switches showed a ~3-fold change in cytoplasmic/nuclear prot we observe. They also observed similar kinetics of nuclear import and export in mammalian cells with half

We are aware of no reports of light activated transcription in *C*. *elegans* and only four studies that demons transcription in multicellular organisms [38–41]. Most showed activation of specific ectopic reporter genes of a DNA binding region in the promoter of the gene of interest. This approach is limited to the activation o at a time. Only one study demonstrates transcriptional activation of an endogenous gene in a living organi Cry2 and CIB1 light dimerization coupled with TALE DNA-binding domain [41]. We created a single compo switch, which allowed us to apply CRISPR/Cas9-triggered homologous recombination for direct, single-ste endogenous transcription factor and, we infer based on resulting phenotypes, its set of gene targets. Cons to trigger a systemic cellular response and control cell fate specification in *C*. *elegans*, opening a wide ran research.

Materials and Methods

DNA cloning

All cloning PCR amplifications were performed using high-fidelity Q5 polymerase and all preliminary const out by colony PCR using Taq polymerase. All enzymes were purchased from New England Biolabs (NEB) verified by DNA sequencing (GeneWiz).

Light illumination setup

The illumination setup for the fluorescence polarization assays was as described in Lungu et al, 2012. Brie with maximum emission at 455 nm (Thorlabs) provided 6 mW/cm^2 illumination to a sample in a 1 cm quar

For the *S*. *cerevisae* and *C*. *elegans* experiments, a LED strip with maximum emission at 465 nm (Mouser 901-SB-0465-CT) was placed in an array 25 x 35 cm, 15 cm above the samples in an incubator set at 30° *C*. *elegans*, thus obtaining even illumination of ± 500 μW/cm^2 for yeast and ± 250 μW/cm^2 for *C*. *elegans*.

Protein expression

Avena sativa phototropin-1 gene corresponding to residues 404–546 encoding for the LOV2 domain (Unip amplified with two-step overlap extension PCR introducing the designed nuclear localization signal and clo BamHI and HindIII restriction digest. The resulting plasmid was transformed in BL21 (DE3) pLysS and bac Bertani media till reaching OD_{600} ~ 0.6 upon which protein production was induced with 500 mM IPTG ove Cell pellets were resuspended in 50 mM Tris pH 7.5, 1 M NaCl, 10 mM Imidazole, 10 mM β-ME and 1 mM 15 mins (5 sec. ON, 5 sec. OFF) on ice at 4°C. Lysed cells were then centrifuged for 30 min at 18564 RCF filtered through 5 μM filter and loaded on 5 mL HisTrap IMAC columns (GE Healthcare). The columns wer 50 mM Tris pH 7.5, 1 M NaCl, 10 mM Imidazole, 10 mM β-ME and eluted on BioLogic LP (BioRad) using a Tris pH 7.5, 100 mM NaCl, 500 mM Imidazole, 10 mM β-ME. The eluted protein was concentrated with An to 2 mL and subjected to size exclusion chromatography in 50 mM Tris pH 7.5, 100 mM NaCl and 1 mM D Superdex 75 (GE Healthcare) run on Akta FPLC (Amersham). Importins were expressed and purified in th above. After IMAC the proteins were concentrated to 5 mL, dialyzed against 5 L of 50 mM Tris pH 7.5 ove over HiTrap Q HP column (GE Healthcare) eluted over a gradient against 50 mM Tris pH 7.5 and 1 M NaC were concentrated to 5 mL and subjected to size exclusion chromatography in 50 mM Tris pH 7.5, 100 mM with HiLoad 16/600 Superdex 200 (GE Healtchare). All protein concentrations were determined using the manufacture protocol (Thermo Scientific Pierce).

Fluorescence polarization

Peptide of the following sequence GDMAAKRVKLD was synthesized at UNC- Chapel Hill and amine labe 6-Carboxytetramethylrhodamine (TAMRA) dye. Peptide concentration was determined by measuring absc dye at 555 nm using 65,000 M^{-1} cm^{-1} as extinction coefficient. All fluorescence polarization measurements FluoroMax3 (Jobin Ybon Horiba) fluorescence spectrometer using 25 nM of the TAMRA labelled peptide in 7.5, 100 mM NaCl and 1 mM DTT. The dye was excited with polarized light at 555 nm and polarization of e 584 nm. The sample was held in a 1 cm quartz cuvette at 25°C, increasing concentrations of importin α we polarization values for dark and lit state binding were recorded for each titration point. The polarization val was collected after 2 minutes of blue light illumination and for the dark state by another measurement take absence of light for the same titration point. Finally, the competition was fit for one-site total binding with P IC50 values were used to determine the Kd with the online calculator [42].

Mammalian cell culture

HeLa, Cos7 HEK293T (ATCC) tissue cultures were grown at 37°C, 10% CO_2 in DMEM supplemented with Standard Fetal Bovine Serum (Thermo Scientific) and 1% (v/v) GlutaMAX (GIBCO). Cells were passaged Nunc T-25 or T-75 culture flasks (Thermo Scientific).

Mammalian cell imaging

Constructs consisting of mCherry and AsLOV2cNLS with or without NES signals located between mCherr cloned in pTriEx with restriction digest cloning using NcoI and HindIII restriction sites. All constructs were s

Coverslips were washed with PBS (GIBCO) and coated with 10 μg/ml fibronectin at room temperature for Cells were seeded for a minimum of 3 hours to overnight, then transfected using FuGENE 6 (Promega) ar hours post-transfection in Ham's F-12K medium free of Phenol red (Caisson) and containing 10% FBS bu HEPES pH 8. Coverslips were mounted in an Attofluor live cell chamber (Invitrogen) placed in a microscop stage adaptor (Warner) and an objective temperature controller (Bioptechs).

An Olympus DSU-IX81 Spinning Disk Confocal coupled with Andor solid-state lasers (Andor) was used to export signal screen. Z-stacks of 12 μm at 0.5 μm steps were acquired with a PlanApo 60× objective (Oil, nm laser set at 20% intensity (150 EM gain and 300 ms exposure).

Live cell timelapse series were collected with an Olympus IX81 epifluorescence microscope equipped with compensator and a Photometrics CoolSnap ES2 CCD camera (Roper Photometrics). A UPlanFLN 40× ob was used with an ET572/35x filter for mCherry detection and 1% (UVND 2.0, ET430/24x) for blue light act

Yeast transcription

LANS4 was amplified and cloned into pNIA-CEN-MBP plasmid [28] using EcoRI and BamHI restriction site was transformed via high efficiency lithium acetate transformation [43] and plated on SC-Leucine droupou

Survival assays were performed as follows: Fresh colonies were grown overnight at 30°C in 5 ml SC-Leuc cell density was measured at OD_{600} and cultures diluted in 200 μl of OD_{600} = 1, followed by 8 5-fold serial each of the dilutions were pipetted and spotted using a multichannel pipette (Gilson) onto respective dropo condition plates were wrapped in aluminium foil and placed in the same incubator as the lit condition at 30 500 μW/cm^2 was provided with LED strip lights attached at the incubator (look at illumination settings). Ye after 72h incubation using an HP ScanJet 4850 scanner and resulting images were cropped and arranged

β-Galactose assay were performed as follows: Fresh colonies were grown overnight at 30°C in 5 ml SC-L the cell density was measured at OD_{600} and 2 mL cultures were diluted to OD_{600} = 0.2 in duplicates—one for a dark condition (falcon tubes were wrapped in aluminium foil). Cultures were grown at 30°C in a shaki reaching OD_{600} ± 0.8 in presence or absence of blue light (465 nm) at 500 μW/cm^2 via LED strip light wra rack. The resulting cultures were pelleted in triplicates and β-Galactose assay using CPRG for a substrate according to the manufacturer (Clontech).

C. elegans culture and strain construction

S1 Table lists the *C. elegans* strains used in this study including the native N2 [44]. All strains were mainta NGM medium, using *E. coli* strain OP50 as a food source. To express mKate2::LANS4 ubiquitously in earl mKate2::LANS4 coding sequence was designed using optimal *C. elegans* codons and synthetic introns [4 assembled from gBlocks gene fragments (Integrated DNA Technologies) using Gibson assembly (New En cloned into a modified pCFJ352 vector [46] containing the *his-72* promoter and *tbb-2* 3'UTR. This construc single-copy transgene into the *ttTi4348* locus on LG I using MosSCI [46]. To express mKate2::LANS4 in M carrying the mKate2::LANS coding sequence was cloned into a modified pCFJ151 vector [46] containing t *tbb-2* 3'UTR. This construct was injected into wild type worms (strain N2) to generate extrachromosomal a

To insert LANS1 into the *lin-1* locus, we used Cas9-triggered homologous recombination [36]. S4 Fig shov gene targeting strategy. We modified the Cas9–sgRNA expression plasmid pDD162 by inserting the guide ATGACGTCGTGGAGGGCGATA. Next, we constructed a homologous repair template by first cloning a 3. comprising the last 3.3 kb of the *lin-1* gene followed by a 0.2 kb intergenic region and the first 0.5 kb of the gene, into the pCR-Blunt TOPO vector. We made 4 modifications to this construct: 1) We deleted a 1 kb fr last 270 bp of *lin-1* coding sequence and an intervening intron, and replaced this fragment with the mKate sequence. 2) We mutated the putative NLS sequence RQCRKRSL to AQCAAASL. 3) We inserted a selec a hygromycin resistance gene [48] followed by *unc-58(n495)*, into the intergenic region downstream of the intended to use the dominant Unc-58 phenotype as a visible marker for the *lin-1* allele, but animals genera do not have an Unc-58 phenotype, indicating that, although *unc-58(n495)* is a dominant mutation, insertio *unc-58(n495)* into an *unc-58(+)* background is not sufficient to cause the Unc-58 phenotype. 4) Finally, be close together and located on the same strand, it is possible that the *lin-1* 3'UTR contains sequences that of *M70.5*, and that insertion of the selectable marker in the intergenic region between *lin-1* and *M70.5* coul expression. To avoid this, we inserted a second copy of the *lin-1* 3'UTR downstream of the selectable mar final homologous repair template is available upon request.

The *elk-2* gene of *C. elegans* has >90% nucleotide sequence identity to the region of *lin-1* that we wished impossible to identify a Cas9 target site that was unique to *lin-1*. Therefore, to avoid inadvertently modifyir we performed Cas9-triggered homologous recombination in the parent strain VC2110, which carries a del removes part of the region homologous to *lin-1*, including the Cas9 target site that we selected. An injectio ng/μL Cas9–sgRNA plasmid, 10 ng/μL homologous repair template, and co-injection markers [36] was inje adults. The injected animals were allowed to lay eggs for 3 days at 25°C, and then hygromycin was added concentration of 0.5 mg/mL to kill non-transformed animals. After 7 days of selection, the plates were heat to kill animals carrying extrachromosomal arrays (via PEEL-1 negative selection [46]). Candidate *lin-1*::*lan* both rounds of selection were singled to establish lines, and correct insertion of *lans* was confirmed by PC remove the unlinked *elk-2* mutation that facilitated strain construction.

Photoactivation experiments in *C. elegans* embryos

Embryos expressing mKate2::LANS4 were mounted on polylysine-coated coverslips and gently flattened u
For whole-embryo photoactivation experiments (Fig 5B), we used a Nikon Eclipse Ti microscope equippec
objective and a Yokagawa CSU-X1 spinning disk head and controlled using Metamorph (Molecular Device
mKate2 fluorescense were captured every 10s, and the embryos were illuminated with ~180 μW/cm^2 of bl
laser for 5s between each pair of image acquisitions (i.e., 50% photoactivation duty ratio). For single-cell p
experiments (Fig 5C), we used a Zeiss LSM710 laser scanning confocal microscope equipped with a 100
controlled by Zeiss Zen software. Images were acquired at 10s intervals, and photoactivation was done be
acquisitions by scanning a 458 nm laser at ~170 W/cm^2 over a region of interest defined using the FRAP/
of the Zen software. Each pixel was illuminated for a total of 63 μs during photoactivation.

To measure mKate2::LANS4 nuclear localization, we made line scans across a region of the image that er
and cytoplasm of each cell of interest. Pixel intensities were measured from kymographs and converted to
subtracting off-embryo background. To correct for photobleaching, we normalized each measurement to th
fluorescence intensity of the entire image.

Scoring of vulval phenotypes

Animals were synchronized by allowing embryos to hatch in the absence of food and arrest as L1 larvae. S
plated on NGM plates seeded with *E. coli* OP50, and the plates were placed under blue LED illumination (
were placed in the same incubator and wrapped in aluminium foil to prevent light exposure. When the anir
stage (approximately 48 hours), they were mounted on 2.5% agar pads containing 10 mM sodium azide a
of the developing vulva were acquired using a Nikon Eclipse E800 microscope equipped with Nomarski op
objective. Animals were scored as Normal if there was a single, symmetric vulval invagination; as Multivul
one secondary invagination in addition to the main vulva; as “weak Vulvaless” if, instead of a fully formed v
were two small, equally-sized invaginations separated by apparently undifferentiated tissue; as Vulvaless i
invagination; and as Deformed if there was a single vulval invagination that was misshapen or asymmetric
was too abnormal to be confidently assigned to one of the other categories. Data were plotted and p value
Graphpad Prism software.

Accession codes

Addgene: pTriEx-mCherry::LANS1, 60784; pTriEx-mCherry::LANS4, 60785.

Supporting Information

S1 Fig. LANS computational design.

(A) Rosetta model of the designed NLS on yeast karyopherin (B) Rosetta model of the chimeric AsLOV2c
doi:10.1371/journal.pone.0128443.s001
(TIF)

S2 Fig. Biophysical characterization of LANS.

(A) Peptide binding to importin α 5 and (B) importin α 7 (C) AsLOV2 native sequence does not compete w
α 5 and α 7 in neither dark nor light conditions (D) Fusing the Myc NLS directly at the C-terminus of AsLO
546 leads to tight but light independent binding to importin α 5 with affinities measured at about 1 nM. (E)
preserves wild type AsLOV2 reversion kinetics.
doi:10.1371/journal.pone.0128443.s002
(TIF)

S3 Fig. LANS is actively exported and tolerates small and large C-terminal fusions.

(A) Treatment with 200 nM of Leptomycin B for 10 minutes reverts the nuclear/cytoplasmic distribution of l
one without a nuclear export signal. Confocal microscopy with a single nuclear optical slice (scale bar 15 μ

of a short peptide (flag tag) and large globular protein (MBP) constructs. (C) Epifluorescent microscopy fo
dark and after 10 minutes of blue light activation (scale bar 25 μm).
doi:10.1371/journal.pone.0128443.s003
(TIF)

S4 Fig. Cas9-triggered homologous recombination schematic.

Schematic of our strategy for modifying the *lin-1* locus using Cas9-triggered homologous recombination. S
procedures for details.
doi:10.1371/journal.pone.0128443.s004
(TIF)

S1 Movie. mCherry::LANS4 blue light activation and reversion in HeLa.

Still images from this movie are shown in Fig 4A. The scale is provided with a scale bar = 25 μm, the time
“ON” indicates intermittent blue light activation (see Supplemental experimental procedures).
doi:10.1371/journal.pone.0128443.s005
(MOV)

S2 Movie. mCherry::LANS4 blue light activation and reversion in Cos7.

Still images from this movie are shown in Fig 4B. The scale is provided with a scale bar = 25 μm, the time
“ON” indicates intermittent blue light activation (see Supplemental experimental procedures).
doi:10.1371/journal.pone.0128443.s006
(MOV)

S3 Movie. mCherry::LANS4 blue light activation and reversion in HEK293.

The scale is provided with a scale bar = 25 μm, the time is shown as min:sec and “ON” indicates intermitte
(see S1 Text).
doi:10.1371/journal.pone.0128443.s007
(MOV)

S4 Movie. Whole-embryo photoactivation of ubiquitously expressed mKate2::LANS4.

Still images from this movie are shown in Fig 5B.
doi:10.1371/journal.pone.0128443.s008
(MOV)

S5 Movie. Photoactivation of mKate2::LANS4 in a single MS cell.

Still images from this movie are shown in Fig 5C.
doi:10.1371/journal.pone.0128443.s009
(MOV)

S1 Table. *C. elegans* strains used in this study.

doi:10.1371/journal.pone.0128443.s010
(XLSX)

S1 Text. Supporting Materials and Methods.

doi:10.1371/journal.pone.0128443.s011
(PDF)

Acknowledgments

We would like to thank Dr. Darren Hart for plasmids encoding human importin α5 and α7; Dr. Chandra Tuc strain; Dr. Joe S. Mymryk for the pNIA-CEN-MBP plasmid; Drs. Josh Kelley and Tony Perdue as well as M microscopy and Drs. David Reiner and Andrianna Beltran for helpful discussions.

Author Contributions

Conceived and designed the experiments: HY DJD HW SPZ JEB BG KH BK. Performed the experiments: Analyzed the data: HY DJD HW SPZ JEB BG KH BK. Wrote the paper: HY DJD BG KH BK.

References

1. Cartwright P, Helin K. Nucleocytoplasmic shuttling of transcription factors. Cell Mol Life Sci. 2000;57(8–9):1193–206. pmid:
View Article • PubMed/NCBI • Google Scholar

2. Eilers M, Picard D, Yamamoto KR, Bishop JM. Chimaeras of myc oncoprotein and steroid receptors cause hormone-deper Nature. 1989;340(6228):66–8. pmid:2662015
View Article • PubMed/NCBI • Google Scholar

3. Feil R, Brocard J, Mascrez B, LeMeur M, Metzger D, Chambon P. Ligand-activated site-specific recombination in mice. Pro 1996;93(20):10887–90. pmid:8855277
View Article • PubMed/NCBI • Google Scholar

4. Metzger D, Clifford J, Chiba H, Chambon P. Conditional site-specific recombination in mammalian cells using a ligand-dep recombinase. Proc Natl Acad Sci U S A. 1995;92(15):6991–5. pmid:7624356
View Article • PubMed/NCBI • Google Scholar

5. Haruki H, Nishikawa J, Laemmli UK. The anchor-away technique: rapid, conditional establishment of yeast mutant phenoty 2008;31(6):925–32. doi: 10.1016/j.molcel.2008.07.020. pmid:18922474
View Article • PubMed/NCBI • Google Scholar

6. Toettcher JE, Voigt CA, Weiner OD, Lim WA. The promise of optogenetics in cell biology: interrogating molecular circuits in 2011;8(1):35–8. doi: 10.1038/nmeth.f.326. pmid:21191370
View Article • PubMed/NCBI • Google Scholar

7. Leifer AM, Fang-Yen C, Gershow M, Alkema MJ, Samuel AD. Optogenetic manipulation of neural activity in freely moving Methods. 2011;8(2):147–52. doi: 10.1038/nmeth.1554. pmid:21240279
View Article • PubMed/NCBI • Google Scholar

8. Wu MC, Chu LA, Hsiao PY, Lin YY, Chi CC, Liu TH, et al. Optogenetic control of selective neural activity in multiple freely n Natl Acad Sci U S A. 2014;111(14):5367–72. doi: 10.1073/pnas.1400997111. pmid:24706830
View Article • PubMed/NCBI • Google Scholar

9. Del Bene F, Wyart C. Optogenetics: a new enlightenment age for zebrafish neurobiology. Dev Neurobiol. 2012;72(3):404–1 pmid:21567983
View Article • PubMed/NCBI • Google Scholar

10. Engelke H, Chou C, Uprety R, Jess P, Deiters A. Control of Protein Function through Optochemical Translocation. ACS Sy

11. Gautier A, Nguyen DP, Lusic H, An W, Deiters A, Chin JW. Genetically encoded photocontrol of protein localization in mam 2010;132(12):4086–8. doi: 10.1021/ja910688s. pmid:20218600
View Article • PubMed/NCBI • Google Scholar

12. Yang X, Jost AP, Weiner OD, Tang C. A light-inducible organelle-targeting system for dynamically activating and inactivatin Mol Biol Cell. 2013;24(15):2419–30. doi: 10.1091/mbc.E13-03-0126. pmid:23761071
View Article • PubMed/NCBI • Google Scholar

13. Niopek D, Benzinger D, Roensch J, Draebing T, Wehler P, Eils R, et al. Engineering light-inducible nuclear localization sign control of protein dynamics in living cells. Nat Commun. 2014;5:4404. doi: 10.1038/ncomms5404. pmid:25019686
View Article • PubMed/NCBI • Google Scholar

14. Lungu OI, Hallett RA, Choi EJ, Aiken MJ, Hahn KM, Kuhlman B. Designing photoswitchable peptides using the AsLOV2 do 2012;19(4):507–17. doi: 10.1016/j.chembiol.2012.02.006. pmid:22520757
View Article • PubMed/NCBI • Google Scholar

15. Strickland D, Lin Y, Wagner E, Hope CM, Zayner J, Antoniou C, et al. TULIPs: tunable, light-controlled interacting protein ta Methods. 2012;9(4):379–84. doi: 10.1038/nmeth.1904. pmid:22388287
View Article • PubMed/NCBI • Google Scholar

16. Yi JJ, Wang H, Vilela M, Danuser G, Hahn KM. Manipulation of Endogenous Kinase Activity in Living Cells Using Photoswi ACS Synth Biol. 2014.

17. Hodel AE, Harreman MT, Pulliam KF, Harben ME, Holmes JS, Hodel MR, et al. Nuclear localization signal receptor affinity localization in Saccharomyces cerevisiae. J Biol Chem. 2006;281(33):23545–56. pmid:16785238
View Article • PubMed/NCBI • Google Scholar

18. Harper SM, Christie JM, Gardner KH. Disruption of the LOV-Jalpha helix interaction activates phototropin kinase activity. B 2004;43(51):16184–92. pmid:15610012
View Article • PubMed/NCBI • Google Scholar

19. Paine PL, Moore LC, Horowitz SB. Nuclear envelope permeability. Nature. 1975;254(5496):109–14. pmid:1117994
View Article • PubMed/NCBI • Google Scholar

20. Wang R, Brattain MG. The maximal size of protein to diffuse through the nuclear pore is larger than 60kDa. FEBS Lett. 200 pmid:17588566
View Article • PubMed/NCBI • Google Scholar

21. Wen W, Meinkoth JL, Tsien RY, Taylor SS. Identification of a signal for rapid export of proteins from the nucleus. Cell. 1995
View Article • PubMed/NCBI • Google Scholar

22. Stommel JM, Marchenko ND, Jimenez GS, Moll UM, Hope TJ, Wahl GM. A leucine-rich nuclear export signal in the p53 te regulation of subcellular localization and p53 activity by NES masking. EMBO J. 1999;18(6):1660–72. pmid:10075936
View Article • PubMed/NCBI • Google Scholar

23. Roth J, Dobbelstein M, Freedman DA, Shenk T, Levine AJ. Nucleo-cytoplasmic shuttling of the hdm2 oncoprotein regulate via a pathway used by the human immunodeficiency virus rev protein. EMBO J. 1998;17(2):554–64. pmid:9430646
View Article • PubMed/NCBI • Google Scholar

24. Watanabe M, Masuyama N, Fukuda M, Nishida E. Regulation of intracellular dynamics of Smad4 by its leucine-rich nuclea 2000;1(2):176–82. pmid:11265759
View Article • PubMed/NCBI • Google Scholar

25. van Hengel J, Vanhoenacker P, Staes K, van Roy F. Nuclear localization of the p120(ctn) Armadillo-like catenin is countera and by E-cadherin expression. Proc Natl Acad Sci U S A. 1999;96(14):7980–5. pmid:10393933
View Article • PubMed/NCBI • Google Scholar

26. Jang BC, Muñoz-Najar U, Paik JH, Claffey K, Yoshida M, Hla T. Leptomycin B, an inhibitor of the nuclear export receptor C expression. J Biol Chem. 2003;278(5):2773–6. pmid:12468543
View Article • PubMed/NCBI • Google Scholar

27. Holt JE, Ly-Huynh JD, Efthymiadis A, Hime GR, Loveland KL, Jans DA. Regulation of Nuclear Import During Differentiation and Spermatogenesis. Curr Genomics. 2007;8(5):323–34. doi: 10.2174/138920207782446151. pmid:19384428
View Article • PubMed/NCBI • Google Scholar

28. Marshall KS, Zhang Z, Curran J, Derbyshire S, Mymryk JS. An improved genetic system for detection and analysis of prote Mol Biol. 2007;8:6. pmid:17254328
View Article • PubMed/NCBI • Google Scholar

29. Ooi SL, Priess JR, Henikoff S. Histone H3.3 variant dynamics in the germline of Caenorhabditis elegans. PLoS Genet. 200
View Article • PubMed/NCBI • Google Scholar

30. Broitman-Maduro G, Owraghi M, Hung WW, Kuntz S, Sternberg PW, Maduro MF. The NK-2 class homeodomain factor CE TBX-35 have overlapping function in C. elegans mesoderm development. Development. 2009;136(16):2735–46. doi: 10.12 pmid:19605496
View Article • PubMed/NCBI • Google Scholar

31. Sternberg PW. Vulval development. WormBook. 2005:1–28.

32. Sulston JE, Horvitz HR. Abnormal cell lineages in mutants of the nematode Caenorhabditis elegans. Dev Biol. 1981;82(1):
View Article • PubMed/NCBI • Google Scholar

33. Ferguson EL, Horvitz HR. Identification and characterization of 22 genes that affect the vulval cell lineages of the nematod Genetics. 1985;110(1):17–72. pmid:3996896
View Article • PubMed/NCBI • Google Scholar

34. Ferguson EL, Sternberg PW, Horvitz HR. A genetic pathway for the specification of the vulval cell lineages of Caenorhabdi 1987;326(6110):259–67. pmid:2881214
View Article • PubMed/NCBI • Google Scholar

35. Jacobs D, Beitel GJ, Clark SG, Horvitz HR, Kornfeld K. Gain-of-function mutations in the Caenorhabditis elegans lin-1 ETS regulatory domain phosphorylated by ERK MAP kinase. Genetics. 1998;149(4):1809–22. pmid:9691039
View Article • PubMed/NCBI • Google Scholar

36. Dickinson DJ, Ward JD, Reiner DJ, Goldstein B. Engineering the Caenorhabditis elegans genome using Cas9-triggered ho Methods. 2013;10(10):1028–34. doi: 10.1038/nmeth.2641. pmid:23995389
View Article • PubMed/NCBI • Google Scholar

37. Strickland D, Yao X, Gawlak G, Rosen MK, Gardner KH, Sosnick TR. Rationally improving LOV domain-based photoswitcl 2010;7(8):623–6. doi: 10.1038/nmeth.1473. pmid:20562867
View Article • PubMed/NCBI • Google Scholar

38. Wang X, Chen X, Yang Y. Spatiotemporal control of gene expression by a light-switchable transgene system. Nat Methods 10.1038/nmeth.1892. pmid:22327833
View Article • PubMed/NCBI • Google Scholar

39. Liu H, Gomez G, Lin S, Lin C. Optogenetic control of transcription in zebrafish. PLoS One. 2012;7(11):e50738. doi: 10.137 pmid:23226369
View Article • PubMed/NCBI • Google Scholar

40. Motta-Mena LB, Reade A, Mallory MJ, Glantz S, Weiner OD, Lynch KW, et al. An optogenetic gene expression system witl deactivation kinetics. Nat Chem Biol. 2014;10(3):196–202. doi: 10.1038/nchembio.1430. pmid:24413462
View Article • PubMed/NCBI • Google Scholar

41. Konermann S, Brigham MD, Trevino AE, Hsu PD, Heidenreich M, Cong L, et al. Optical control of mammalian endogenous states. Nature. 2013;500(7463):472–6. doi: 10.1038/nature12466. pmid:23877069
View Article • PubMed/NCBI • Google Scholar

42. Nikolovska-Coleska Z, Wang R, Fang X, Pan H, Tomita Y, Li P, et al. Development and optimization of a binding assay for fluorescence polarization. Anal Biochem. 2004;332(2):261–73. pmid:15325294
View Article • PubMed/NCBI • Google Scholar

43. Gietz RD, Schiestl RH. High-efficiency yeast transformation using the LiAc/SS carrier DNA/PEG method. Nat Protoc. 2007
View Article • PubMed/NCBI • Google Scholar

44. Brenner S. The genetics of Caenorhabditis elegans. Genetics. 1974;77(1):71–94. pmid:4366476
View Article • PubMed/NCBI • Google Scholar

45. Redemann S, Schloissnig S, Ernst S, Pozniakowsky A, Ayloo S, Hyman AA, et al. Codon adaptation-based control of prote Nat Methods. 2011;8(3):250–2. doi: 10.1038/nmeth.1565. pmid:21278743
View Article • PubMed/NCBI • Google Scholar

46. Frøkjær-Jensen C, Davis MW, Ailion M, Jorgensen EM. Improved Mos1-mediated transgenesis in C. elegans. Nat Method 10.1038/nmeth.1865. pmid:22290181
View Article • PubMed/NCBI • Google Scholar

47. Mello CC, Kramer JM, Stinchcomb D, Ambros V. Efficient gene transfer in C.elegans: extrachromosomal maintenance and sequences. EMBO J. 1991;10(12):3959–70. pmid:1935914
View Article • PubMed/NCBI • Google Scholar

48. Greiss S, Chin JW. Expanding the genetic code of an animal. J Am Chem Soc. 2011;133(36):14196–9. doi: 10.1021/ja205
View Article • PubMed/NCBI • Google Scholar